Int. J. Electrochem. Sci., 13 **(2018)** 7385 – 7396, doi: 10.20964/2018.08.09

International Journal of ELECTROCHEMICAL SCIENCE
www.electrochemsci.org

Synthesis, Characterization and Application of Ferrochrome slag/polyaniline Nanocomposite as Corrosion Protection Coatings for Carbon Steel

M.I. Khan[1,*], *A. Amari*[1], *A. Mustafa*[1], *H. Shoukry*[2], *Ismat H. Ali*[3], *Saviour A. Umoren*[4], *A. Madhan Kumar*[4]

[1] Chemical Engineering Department, College of Engineering, King Khalid University, Abha, Saudi Arabia,
[2] Physics Department, College of Science, King Khalid University, Abha, Saudi Arabia
[3] Chemistry Department, College of Science, King Khalid University, Abha, Saudi Arabia
[4] Center of Research Excellence in Corrosion, Research Institute, King Fahd University of Petroleum and Minerals, Dhahran 31261, Saudi Arabia
[*]E-mail: mkaan@kku.edu.sa

Received: 3 April 2018 / *Accepted:* 3 June 2018 / *Published:* 5 July 2018

The corrosion protection ability of waste ferrochrome slag (FeCr-slag) material was investigated. FeCr-slag has been milled for 4 hours in order to obtain nanostructured material. As a nanomaterial, this compound was used as prepared as well as a nanocomposite with polyaniline. The nanocomposites were prepared by in-situ polymerization technique. The prepared materials were characterized by FTIR, XRD and SEM. The anticorrosion performance of FeCr-slag material, polyaniline (PANI) and a nanocomposite of FeCr-slag material with polyaniline was evaluated by incorporating these pigments in a commercial epoxy paint system. The prepared coatings were investigated for their anticorrosion ability by exposure to corrosive media in salt spray chamber as well as the electrochemical potentiodynamic polarization (PDP) and electrochemical impedance spectroscopy (EIS) methods. The results show that the nanocomposite pigments performed better, followed by FeCr-slag material and followed by PANI respectively. Modification of the FeCr-slag material with PANI has significantly improved the anticorrosion properties of the paint system used.

Keywords: carbon steel, corrosion inhibition, FeCr-slag, PANI, nanocomposites

1. INTRODUCTION

Corrosion is a natural phenomenon and has a significant impact on the socio-economic aspects of life. Carbon steel is commonly used as a construction material in various applications such as in

construction, transportation, pipeline etc. However, the life span of carbon steel like many other materials is limited primarily due to corrosion. To overcome this issue, the use of various types of commercially available anticorrosion paints and inhibitors are being introduced into the market. However, researchers and scientists are always on the outlook for more efficient, cheaper and environmental friendly coatings and inhibitors. Among the conductive polymers, polyaniline is probably the one of the oldest synthetic conductive polymer [1]. It is the green protonated emeraldine base that exhibits the conductive form of polyaniline [2]. The exact mechanism of protection offered by conductive polymers is still not clear but one of the most commonly accepted mechanism is the surface ennobling and anodic passivation of the steel surface induced by the inherent redox capability of conductive polymers. Another recently proposed mechanism of protection is the so called self-healing mechanism in which doping the conductive polymers with suitable anionic inhibitors can act as a reservoir of corrosion inhibitors [3].

Protective coatings are commonly used to protect steel structures against corrosion. The use of organic-inorganic composites or hybrid materials have proven to be effective because it combines the various attractive properties such as flexibility, ductility and dielectric of organic as well as the desirable properties such as thermal stability, strength and hardness etc. of the inorganic constituent [4]. The use of conductive polymers modified inorganic nanoparticles are also known to improve the physical properties of materials [5]. These types of modified pigments are capable of providing the highest level of protection against corrosion. The use of polyaniline modified anticorrosive pigments include; polyaniline-SiO_2 composite [6-7], polyaniline-Fe_2O_3 composite coatings [8], polyaniline-ZnO-epoxy composite coatings [9], polyaniline–TiO_2 composite containing coatings [10], polyaniline glass flake composite coatings [11] and various other inorganic pigments as corrosion inhibitors [12]. The current research is focusing on investigating the use of waste slag material (FeCr-slag) from ferrochrome industry as corrosion inhibitor for carbon steel. The surface of these pigments will be modified by treatment with polyaniline. The anti-corrosion efficiency will be evaluated both for the untreated pigments and for the pigments modified with polyaniline. The use of this material as a corrosion inhibitor is scarce in literature and therefore is the focus of the current research.

2. EXPERIMENTAL

2.1 Materials

The ferrochrome slag waste material was taken from a steel manufacturing facility in Oman. The solid waste slag material was ball milled for 4 hours to convert it into a nanostructured material. Hydrochloride and ammonium peroxy disulphate (APS) was purchased from Sigma Aldrich and used without any modifications. Carbon steel coupons and the paint (epoxy zinc rich primer) were provided by Aljazeera Paint Company.

2.2 Preparation of PANI-FeCr-slag Nanocomposite

Aniline hydrochloride (2.59g) was dissolved in distilled water in a 50 ml volumetric flask. Also, ammonium peroxy disulphate (5.71g) was dissolved in a 50 ml volumetric flask. Both solutions were kept in an ice-cold bath for 1 hour. Pre-cooled APS solution was added dropwise to the aniline hydrochloride solution while constantly stirred using a magnetic stirrer. The nanocomposite material with PANI was prepared in similar manner except that the FeCr-slag was added during the mixing and polymerization process. After the complete addition of APS solution, stirring was allowed to continue for another two hours in order to achieve complete polymerization. The mixture was then filtered, washed several times with distilled water to neutralize the pH. The solid filtrate was dried in the oven at 60^0C for 24 hours followed by grinding in a mortar and sieved to size of less than 126 µm.

2.3. Preparation of the coating formulations

Epoxy zinc rich phosphate primer was used. The prepared pigments as nanomaterials incorporated into the primer were 1% by weight. Three nanomaterials namely PANI (sample A), FeCr-slag material (sample B), nanocomposite (C) were tested. These materials were blended into the primer using commercial blender in a paint manufacturing facility. Salt spray coating technique was employed to apply the blended coatings on carbon steel coupons. The finished coated samples were allowed to cure for 7 days prior to salt spray testing.

2.4. Characterization of the prepared nano pigments

The structure of the synthesized polymer and composites was characterized by means of an IR spectrometry (TA instrument with universal ATR attachment, range 400–4000 cm^{-1}). As for the X-ray Diffractometer (Rigaku, Japan) using Cu Kα radiation (λ = 0.15406 Å) with operating voltage of 40 kV and current of 30 mA was employed to examine the phase and crystal structure identification in a 2θ range from 10 to 80°. Surface morphologies of synthesized polymer and composite samples were analyzed using Scanning electron microscopy (JSM-6360, JEOL) at an acceleration voltage of 20 kV and irradiation current of 10 µA.

2.5. Characterization of the coated steel panels

2.5.1 Dry film thickness measurements

Dry film thickness measurements were carried out according to ISO 19840 using commercial coating thickness meter (from Paint Test Equipment). Thickness measurements were conducted at five different points and the average values are used in the final evaluation. The results are presented in Table 1. As can be seen, the coated thickness on the three samples is relatively uniform and in close agreement with each other.

Table 1. Dry film thickness measurements of the coated samples (µm)

	A (PANI)	B (FeCr-slag)	C (Nanocomposite)
1	38	39	48
2	44	43	55
3	28	37	39
4	31	41	48
5	41	35	34
Average	**36**	**39**	**45**

2.5.2 Exposure in Salt Spray Chamber

The coated steel coupons were subjected to salt spray testing conditions in accordance with ASTM B117. Salt spray testing method provides a controlled corrosive environment that has been utilized to produce relative corrosion resistance information for the test samples exposed in the test chamber.

2.5.3 Electrochemical testing

Electrochemical corrosion tests were conducted using the Gamry Potentiostat Reference 600 together with Echem analyst software to analyze the experimental data. Conventional three electrode assembly was used to perform the electrochemical experiments in which carbon steel specimen with exposure area of $1cm^2$ acts as working electrode, silver/silver chloride (Ag/AgCl) electrode and graphite rod act as reference and counter electrode respectively. Carbon steel specimens were immersed for about 1 h to check the steady-state prior to each measurement. Potentiodynamic polarization tests were performed at the potential of ±250 mV from open circuit potential (OCP) at a scan rate of 1 mVs^{-1}. Electrochemical impedance spectroscopic tests were monitored over the frequency range of 10^4 to 10 mHz, with acquirement of 10 points per decade and a signal amplitude of 10 mV at OCP. All measurements were repeated at least three times and good reproducibility of the results was observed.

3. RESULTS AND DISCUSSION

3.1 FTIR Analysis

Fig. 1 presents the IR spectra of synthesized PANI, FeCr-slag and its nanocomposite. The obtained peaks at 1462 and 1555 cm^{-1} of PANI are ascribed to the stretching mode of C=C and C=N of benzenoid and quinoid rings, respectively. The peaks at 1287 and 1229 cm^{-1} are accredited to C-N stretching mode of benzenoid ring and peak at 1039 cm^{-1} related to a plane bending vibration of C-H. In the case of IR spectra of ferrochrome nanoparticles, the appeared peaks around 600–400 cm^{-1} are

allocated to Fe-O and Cr-O stretching respectively. The IR spectra of nanocomposite is similar to that of pure PANI when the peaks for C=N, C=C and C-N altogether moved to lower wave numbers (red shift), i.e. 1552, 1455, 1282 and 1224 cm^{-1} due to strong interaction of ferrochrome, which is in good agreement with the previous reports [13-15].

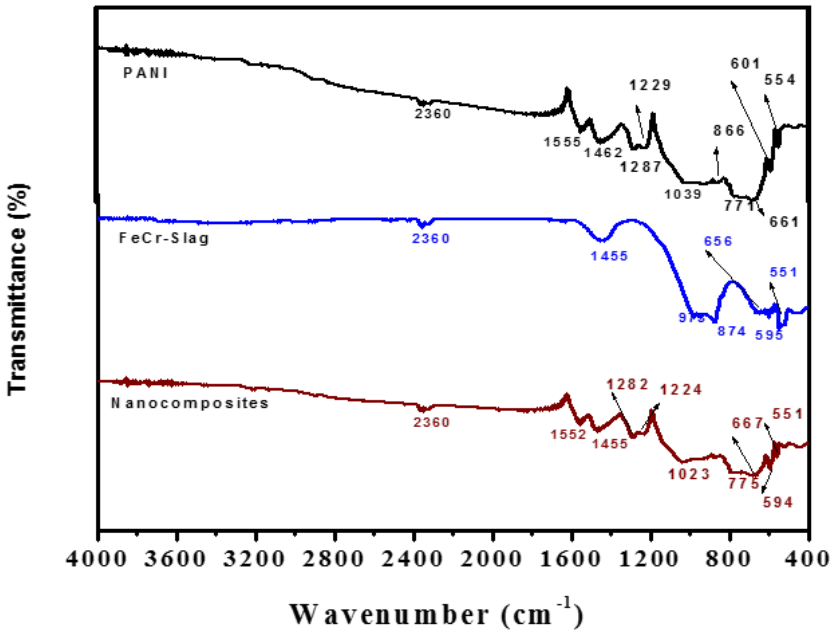

Figure 1. IR spectra of synthesized PANI, FeCr-slag and its nanocomposites

3.2 XRD Analysis

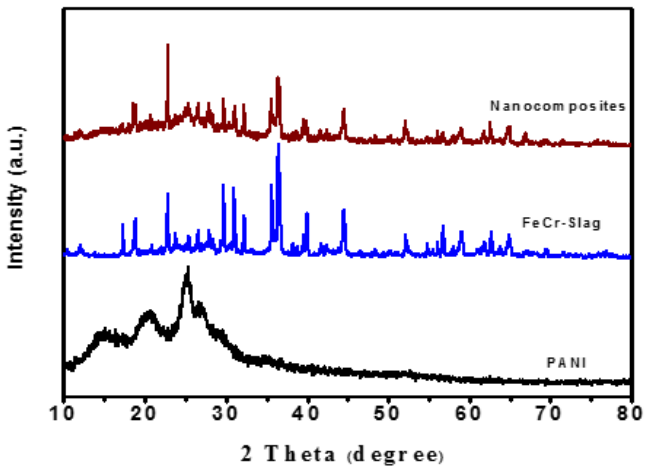

Figure 2. XRD pattern of synthesized PANI, FeCr-slag and its nanocomposites

The XRD data for all the three samples is presented in Figure 2. The XRD pattern obtained for PANI is similar to the one reported by [8] and [9]. The two main Bragg diffraction peaks of PANI

appeared at angles of 2θ = 19.3 and 2θ = 25.7 in the spectrum as reported by [9]. The presence of the rigid aromatic backbone of PANI makes it a semi-crystalline polymer [16]. Peaks of the FeCr-slag has become smaller by the addition of PANI as shown by the spectra of the nanocomposite that confirms the formation of the organic-inorganic nanocomposite.

3.3. SEM Analysis

The SEM micrographs of the prepared PANI, FeCr-slag and FeCr-slag modified PANI nanocomposite are introduced in Figure 3. As it is clear, the PANI showed non-uniform morphology which satisfies its poor crystalline characteristics as confirmed by XRD. Morphology examinations of FeCr-slag indicated that the nanoparticles are homogeneously dispersed with minor agglomeration and have the diameter of about 80–100 nm with spherical morphology. In contrast, the microstructural observation of nanocomposite obviously implies that FeCr-slag nanoparticles are well embedded and strongly held to the PANI matrix, signifying the presence of some interaction between the FeCr-slag nanoparticles and the PANI matrix. Nano-scale particles can be identified in the nanocomposite; these nano particles can effectively distribute through the coating matrix and help in enhancing the corrosion protection efficiency.

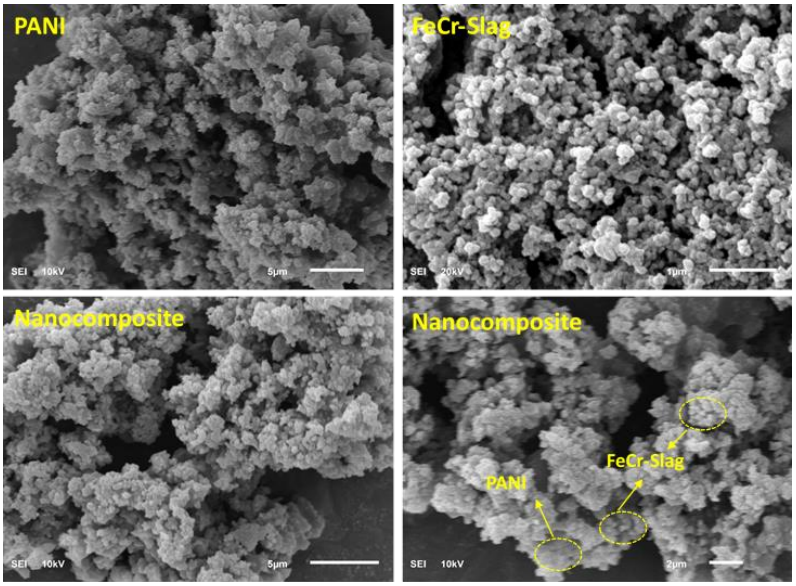

Figure 3. SEM images of synthesized PANI, FeCr-slag and its nanocomposite

3.4. Salt Spray Exposure Test

As shown in Figure 4, visual observations of the specimens after salt spray exposure reveal that the carbon steel (CS) sample coated with the paint containing PANI (sample A) has experienced the most corrosion. The paint system containing the FeCr-slag nanoparticles (sample B) exhibits less corrosion than the PANI system followed by the coating system containing the nanocomposite (sample

C). In other words, the coating system containing the nanocomposite pigment exhibited the least corrosion as anticipated.

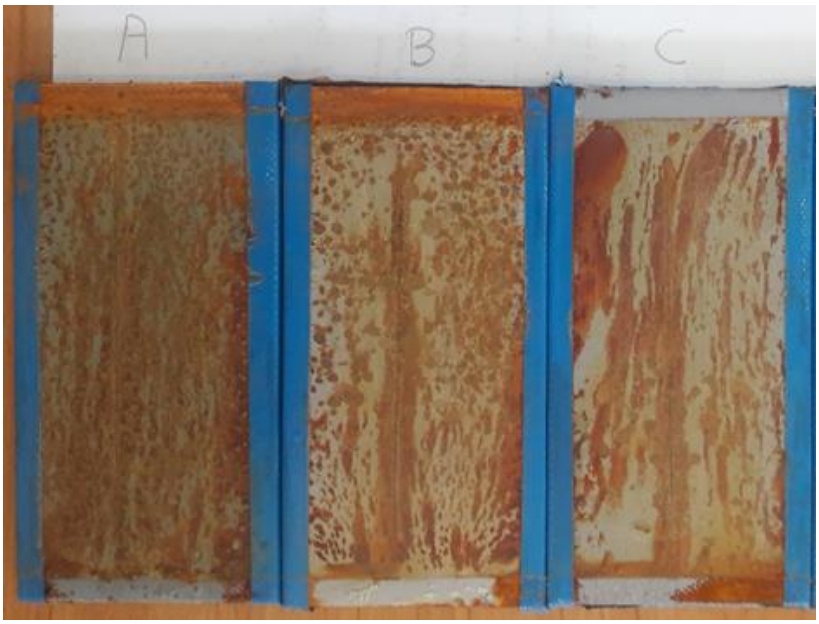

Figure 4. Picture of the coated CS specimens after 8000 hours of exposure in salt spray

3.5 Electrochemical Corrosion Studies

As for the electrochemical results, the typical potentiodynamic polarization results for PANI, FeCr-slag and nanocomposite coated CS specimens in 3.5% NaCl solution at 25 ^{o}C after 24 h immersion are presented in Figure 5. The electrochemical parameters extracted from the Tafel plot analysis are presented in Table 2. The steel specimens with coatings exhibited more positive E_{corr} values compared to that of the bare specimen, indicating that the polymer coatings become a physical barrier for diffusion of aggressive species from solution and improve the corrosion resistance of the steel specimens [17]. In particular, a larger shift of E_{corr} towards nobler direction was observed with an inclusion of nanocomposites into the coatings. Moreover, a significant shift towards lower current densities (i_{corr}) was observed, and particularly, i_{corr} was reduced by about two orders of magnitude. The corrosion rate (CR) was calculated using the i_{corr} values and Eq. (1).

$$CR = 3268 \times i_{corr} \times EW/D \quad (1)$$

where i_{corr} denotes the corrosion current density (mA cm^{-2}), EW and D is the equivalent weight and density (g cm^{-3}) of the specimen, respectively.

Generally, the high corrosion potential along with the low corrosion current density of the coatings specifies a lower corrosion rate with a higher corrosion protection performance [18]. The protection efficiency (PE) of the polymer coatings were calculated using the following expression:

$$PE(\%) = R_p(coated) - R_p(bare) / R_p(coated) \times 100 \quad (2)$$

From equation 2, the PEs obtained are 81.75, 82.95 and 95.79% for PANI, FeCr-slag and nanocomposite samples, respectively. From the obtained results, it is revealed that the addition of PANI into the coatings act as a barrier which restrict the permeation of the electrolyte and also reducing the corrosion rate by participating in the electrochemical reactions. Furthermore, the inclusion of the nanocomposite into the coating matrix could hinder the corrosion process of the CS specimens due to the existence of FeCr-slag nanoparticles within the PANI matrix which might function as a reinforcement network and make a coating which is more compact and corrosion resistant [19].

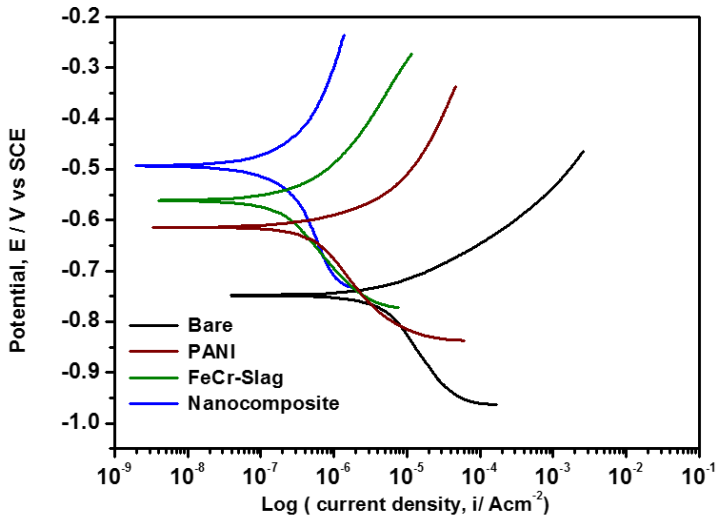

Figure 5. Polarization curves of bare and coated CS specimens after 24 h of immersion in 3.5 % NaCl solution at room temperature with a scan rate of 1 mVs^{-1}

Table 2. Polarization parameters for bare and coated CS samples in 3.5% NaCl at 25 ^{o}C after 24 h immersion

Samples	E_{corr} (mV Vs Ag/AgCl)	I_{corr} $\mu A/cm^2$	βa (mV/dec.)	βc (mV/dec)	CR (mm/yr)	PE (%)
Bare	-748	3.510	158	62	40.69	-------
PANI	-614	0.668	127	73	7.74	81.75
FeCr-slag	-561	0.865	187	98	10.14	82.95
Nanocomposites	-493	0.171	165	75	1.98	95.79

In order to gain further insight into the corrosion protection behavior of PANI and its nanocomposite coated CS specimens, EIS tests were conducted and the results obtained are presented in Figure 6 and 7 in Nyquist and Bode formats respectively. Nyquist diagram of the coated CS specimens exhibited two time constants at low and high frequency regions (Fig. 6), whereas the former

is attributed to the responses of electrolyte/coating interface, the latter is associated with the corrosion processes occurring at the electrolyte/metal interface [20].

Generally, the length of the semicircle arc is related with the polarization resistance (R_p) and therefore the corrosion rate; the lengthier the semicircle arc, the lesser the corrosion rate [21]. Comparing the Nyquist plots of the bare and coated specimens, the coated specimens exhibited the highest R_p. The diameter of the capacitive arc for the nanocomposite coatings is observed to be larger in comparison to others, signifying that the nanocomposite coatings conferred the highest corrosion protection performance on the CS specimens in 3.5% NaCl solution.

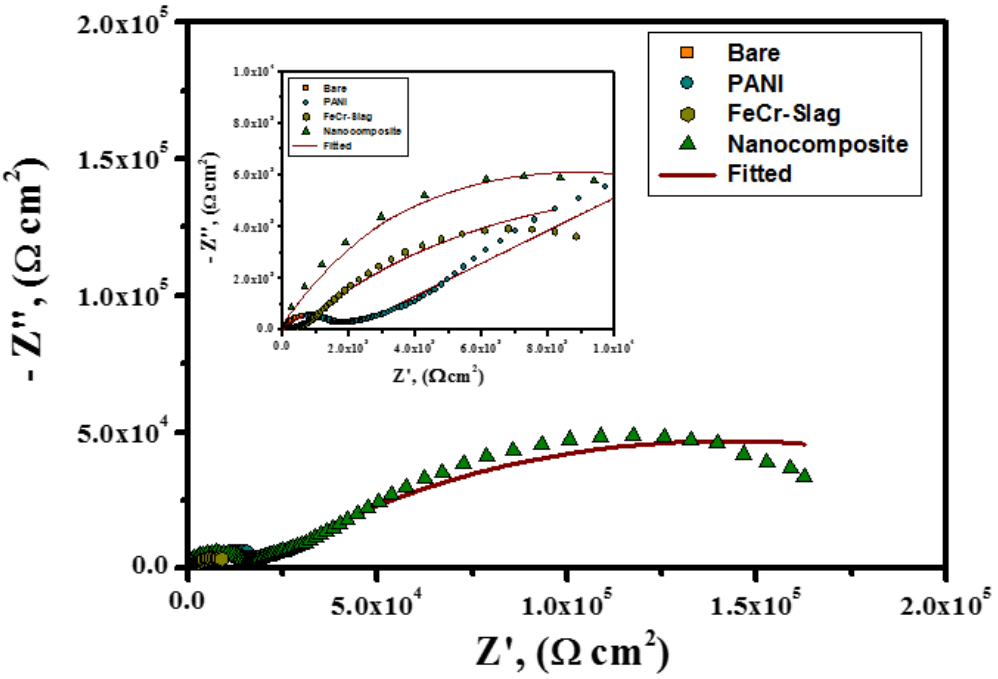

Figure 6. Nyquist plots of bare and coated CS specimens after 24 h of immersion in 3.5 % NaCl solution at room temperature

Bode plots of the bare and coated CS specimens are presented in Figure 7. The impedance parameters of interest was generated by fitting the experimental data into equivalent circuit models, and the achieved fitting values displayed proper reliability with the experimental results. The equivalent circuit models are represented as (Fig. 8a) $Rs(R_{ct}Q_{dl})$ for the bare and (Fig. 8b) $R_s(R_fQ_f)(R_{ct}Q_{dl})$ for the coated specimens, where R_s, R_{ct}, R_f means the solution, charge transfer, and film resistances, respectively, and Q_{dl} and Q_f are the double layer and coating capacitances, respectively [22].

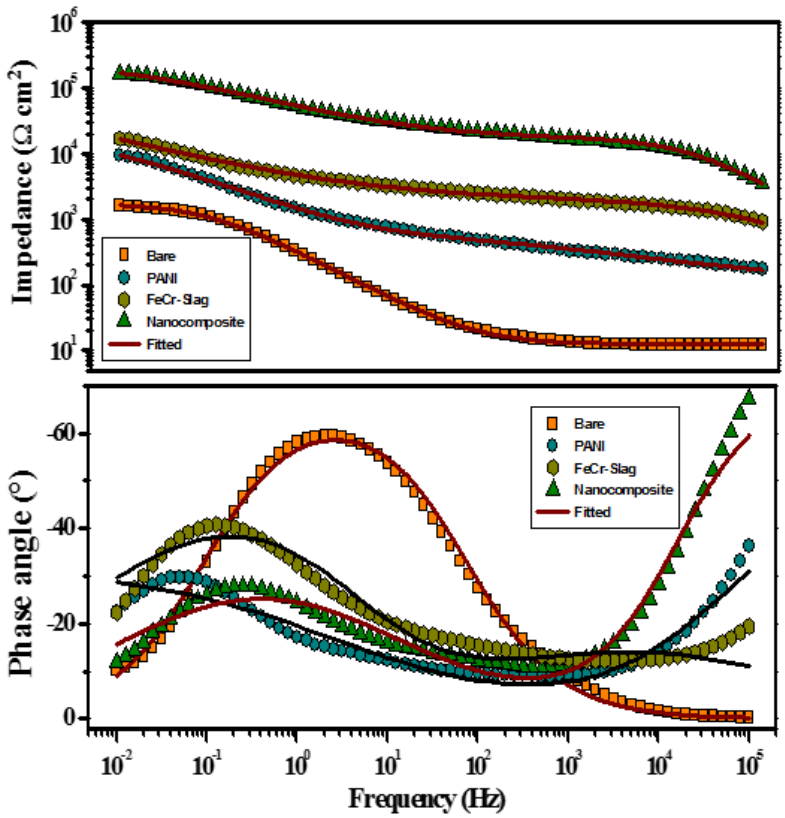

Figure 7. Bode plots of bare and coated CS specimens after 24 h of immersion in 3.5 % NaCl solution at room temperature

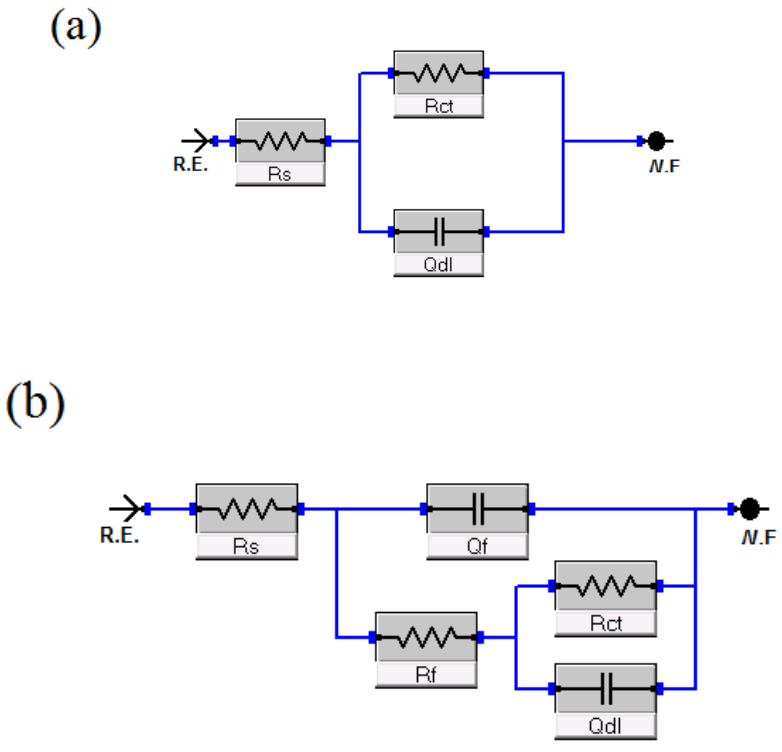

Figure 8. EIS circuit models for (a) bare and (b) coated CS specimens

Constant phase elements (CPE/Q) were used to get the accurate fitting by replacing the capacitive elements in the circuits. The impedance of a CPE can be represented as:

$$Z_{CPE} = [Y_0 (j\,\omega)^n]^{-1}, \quad (3)$$

where Y_0 and n are frequency independent parameters and ω is the angular frequency [21]. The obtained experimental results were well fitted to the theoretical data and the estimated impedance values are listed in Table 3. Generally, the impedance values at the lower frequency region (10 mHz) hold an important part in relating the electrochemical behavior and integral features of the coating at the interface [23]. All of the coatings exhibited a higher impedance value at a lower frequency region compared to that of the bare CS specimen. From the Table 3, the R_{ct} value of the coated CS specimens increased from 1.76 kΩ cm^2 for bare to 9.45, 16.54 and 166.8 kΩ cm^2 for the PANI, FeCr-slag and nanocomposite coated specimens, respectively, representing improved corrosion protection behavior for the coatings.

Generally, R_f values could be influenced by the number of pores/passageway networks in the metallic surface, through which the permeation of corrosive species occurs [24]. The highest R_f value was observed for the specimens coated with nanocomposite, demonstrating that the micro cracks and pores are closed by the reinforcement of nanocomposites. Hence, the inclusion of the nanocomposites seems to significantly decrease the porosity of the coatings by filling the probable micro cracks/cavities inside the coating [25]. Moreover, this performance proficiently hinders and extends the diffuse pathway of aggressive elements, such as Cl^- and H_2O [26]. From the obtained results, it can be concluded that the steel specimens coated with coating formulation containing the nanocomposite display enhanced corrosion protection behavior in 3.5% NaCl solution.

Table 3. EIS parameters for bare and coated CS samples in 3.5% NaCl at 25 ^oC after 24 h immersion

Samples	R_s (Ω cm^2)	R_{ct} (kΩ cm^2)	R_f (kΩ cm^2)	CPE_{dl} (μF cm^{-2})	n_{dl}	CPE_f (μF cm^{-2})	n_f	PE (%)	$\chi^2 \times 10^{-3}$
Bare	28.2	1.76	-----	838.60	0.80	-----	------	------	2.25
PANI	173.3	9.45	2.23	231.65	0.96	99.00	0.94	81.37	3.30
FeCr-slag	152.0	16.54	2.15	180.00	0.94	3.84	0.92	89.35	2.47
Nanocomposite	121.0	166.80	46.96	10.54	0.97	0.74	0.96	98.94	3.21

4. CONCLUSION

In this paper, the anticorrosion performance of three different pigments namely; FeCr-slag nanomaterial, PANI and a nanocomposite of these two materials was evaluated by incorporating these pigments in a commercial epoxy zinc rich phosphate primer. As highlighted in the salt spray exposure

and electrochemical tests, the coating formulation that contain the nanocomposite demonstrate superior corrosion protection properties. The results show that the nanocomposite pigments performed better, followed by the FeCr-slag nanomaterial followed by PANI respectively. As expected, modification of the FeCr-slag nanomaterial (raw material) with conductive polymer PANI has significantly improved the anticorrosion properties of the paint system used.

ACKNOWLEDGEMENT
The author gratefully acknowledges the research funding for this project No.455, provided by Deanship of Scientific Research, King Khalid University, ABHA, KSA. Also, the author would also like to acknowledge the technical support of Engineer Mohamed Al-Zaher from Aljazeera Paints Company in Saudi Arabia.

References

1. J. Prokeš, J. Stejskal and M. Omastová, *Chem. listy*, 95 (2001) 484.
2. J. Stejskal, P. Kratochvíl and A. D. Jenkins, *Polymer*, 37 (1996) 367.
3. T. Niratiwongkorn, G. E. Luckachan and V. Mittal, *RSC Adv*., (2016) 43237.
4. R. Suleiman, H. Dafalla and B.El Ali, *RSC Adv*., (2015) 39155.
5. A. Kalendova, E. Halecka, K. Nechvilova and M. Kohl, *Koroze a ochrana materiálu*, 61 (2017) 39.
6. A. A. Al-Dulaimi, S. Hashim and M.I. Khan, *Sains Malays.*, 40 (2011) 757.
7. G. Ruhi, H. Bhandari and S. K. Dhawan, *Prog. Org. Coat*., 77 (2014) 1484.
8. S. Sathiyanarayanan, S. S. Azim and G. Venkatachari, *Synth. Met*., 157 (2007) 751.
9. A. Mostafaei, and F. Nasirpouri, *Prog. Org. Coat*., 77 (2014) 146.
10. S. Sathiyanarayanan, S. S. Azim and G. Venkatachari, *Prog. Org. Coat*., 59 (2007) 291.
11. S. Sathiyanarayanan, S. S. Azim and G. Venkatachari, *Electrochim. Acta*, 53 (2008) 2087.
12. A. Kalendova, D. Vesely and J. Stejskal, *Prog. Org. Coat*., 62 (2008) 105.
13. M. Kryszawski and J.K. Jezka, *Synth. Met*., 94 (1998) 99.
14. X. Li, G. Wang, X. Li and D. Lu, *Appl. Surf. Sci.*, 229 (2004) 395.
15. C. Wang, Z. Tan, Y. Li, L. Sun and T. Zhan, *Thermochim. Acta*, 441 (2006) 191.
16. L. Shi, X. Wang, L. Lu, X. Yang and X. Wu, *Synth. Met.* 159 (2009) 2525.
17. A. M. Kumar, B. Suresh, S. Ramakrishna and Kye-Seong Kim, *RSC Adv*., 5 (2015) 99866.
18. N. Attarzadeh, K. Raeissi and M.A. Golozar, *Prog. Org. Coat.*, 63 (2008) 167.
19. A. M. Kumar and N. Rajendran, *Ceram. Int*., 39 (2013) 5639.
20. N. Imaz, M. Ostra, M. Vidal, J.A. Díez, M. Sarret and E. García-Lecin, *Corros. Sci*., 78 (2014) 251.
21. Y. Maocheng, A. C. Vetter and J. V. Gelling, *Corros. Sci.*, 70 (2013) 37.
22. A. M. Kumar, Z and M. Gasem, *Surf. Coat. Technol*., 276 (2015) 416.
23. M. Hattori, A. Nishikata and T. Tsuru, *Corros. Sci*., 52 (2010) 2080.
24. P. G. Pawar, R. Xing, R. C. Kambale, A. M. Kumar, S. Liu and S. S. Latthe, *Prog. Org. Coat*., 105 (2017) 235.
25. A. M. Kumar, S. Nagarajan, N. Rajendran and T. Nishimura, *J. Solid State Electrochem*, 16 (2012) 2085.
26. Y. Jafari, S.M. Ghoreishi and M. S. Nooshabadi, *Synth. Met*., 217 (2016) 220.